Hypoxia-induced pathological angiogenesis mediates tumor cell dissemination, invasion, and metastasis in a zebrafish tumor model

Samantha Lin Chiou Lee[a,b,1], Pegah Rouhi[a,1], Lasse Dahl Jensen[a], Danfang Zhang[a], Hong Ji[a], Giselbert Hauptmann[c,d], Philip Ingham[b], and Yihai Cao[a,2]

[a]Department of Microbiology, Tumor and Cell Biology, Karolinska Institute, 171 77 Stockholm, Sweden; [b]Institute of Molecular and Cell Biology, A*STAR, 61 Biopolis Drive Proteos, Singapore 138673; [c]School of Life Sciences, Södertörns University College, 14189 Huddinge, Sweden; and [d]Department of Biosciences and Nutrition, Karolinska Institute, 14157 Huddinge, Sweden

Edited by Robert Langer, Massachusetts Institute of Technology, Cambridge, MA, and approved September 25, 2009 (received for review August 13, 2009)

Mechanisms underlying pathological angiogenesis in relation to hypoxia in tumor invasion and metastasis remain elusive. Here, we have developed a zebrafish tumor model that allows us to study the role of pathological angiogenesis under normoxia and hypoxia in arbitrating early events of the metastatic cascade at the single cell level. Under normoxia, implantation of a murine T241 fibrosarcoma into the perivitelline cavity of developing embryos of transgenic *fli1:EGFP* zebrafish did not result in significant dissemination, invasion, and metastasis. In marked contrast, under hypoxia substantial tumor cells disseminated from primary sites, invaded into neighboring tissues, and metastasized to distal parts of the fish body. Similarly, expression of the hypoxia-regulated angiogenic factor, vascular endothelial growth factor (VEGF) to a high level resulted in tumor cell dissemination and metastasis, which correlated with increased tumor neovascularization. Inhibition of VEGF receptor signaling pathways by sunitinib or VEGFR2 morpholinos virtually completely ablated VEGF-induced tumor cell dissemination and metastasis. To the best of our knowledge, hypoxia- and VEGF-induced pathological angiogenesis in promoting tumor dissemination, invasion, and metastasis has not been described perviously at the single cell level. Our findings also shed light on molecular mechanisms of beneficial effects of clinically available anti-VEGF drugs for cancer therapy.

hypoxia | tumor invasion | VEGF

Angiogenesis not only is essential for primary tumor growth but also facilitates tumor invasion and metastasis (1, 2). Tumor microvascular networks possess several unique pathological features distinguishing them from healthy blood vessels. These include extremely high densities of leaky, tortuous, and primitive microvessels that usually lack pericyte coverage, basement membrane, and arteriole-venule distinctions (3–6). These unusual features often create a hypoxic environment owning to poor blood perfusion, high interstitial fluid pressure (IFP), acidosis, and fast growth as well as metabolic rates of malignant tissues (7, 8). Although hypoxia often results in necrosis of the central core of a fast-growing tumor, it could potentially persuade tumor cells to invade neighboring healthy vasculatures for survival, eventually leading to metastasis, which is one of the hallmarks for cancer therapy (9–13).

Recent studies show that antiangiogenic drugs and vascular destructive agents also promote tumor cell invasion and metastasis in association with drug-induced tumor hypoxia (14–16). However, molecular mechanisms and detailed processes underlying hypoxia-associated metastasis remain poorly understood. A clinical detectable metastatic mass often represents an ultimate consequence of several distinctive steps of the metastatic cascade, including dissemination of malignant cells from the primary site, transport of tumor cells via the circulation or lymphatic system, adhesion of tumor cells in distal tissues/organs, and re-growth of tumor cells into a detectable mass (17). Thus, clinical detection of a metastasis does not reveal early events of tumor cell dissemination and intimate interactions between tumor cells and microvessels. Although various animal models have been established to recapitulate the clinical situation, none of them were designed to study early events of metastasis particularly under tissue hypoxia.

Hypoxia is an effective driving force for angiogenesis, which represents a compensable mechanism against tissue ischemia (18, 19). Hypoxia-induced angiogenesis is mainly mediated by VEGF via activation of the prolyl-hydroxylase-hypoxia inducible factor (HIF) signaling pathway (20, 21). Owing to the hypoxic nature in malignant tumors, virtually all tumors express high levels of VEGF that significantly contributes to high degrees of leakiness and tortuosity of the tumor vasculature. Thus, VEGF-induced neovascularization might promote tumor invasion and metastasis by increasing dissemination of tumor cells into the circulation.

In this study, we show that hypoxia and VEGF significantly contribute to early events of the metastatic cascade. Having developed a hypoxic zebrafish model, we could monitor tumor cell dissemination, invasion, and metastasis in living fish at the single cell level. These findings shed light on mechanisms by which VEGF contributes to tumor invasion and metastasis, and on mechanisms underlying the beneficial effects of clinical available anti-VEGF drugs for the treatment of various human cancers.

Results

Hypoxic Metastasis Model in Zebrafish. To study the role of tissue hypoxia in promoting early events of the metastatic cascade in relation to angiogenesis, we developed a zebrafish tumor model in which the *Tg(fli1:EGFP)* zebrafish embryos (22) were implanted with mouse tumor cells. Murine T241 tumor cells were labeled with DiI dye in vitro and labeled cells were injected into the perivitelline cavity of 48 h post-fertilization embryos (Fig. S1). Tumor-bearing zebrafish embryos were placed in either normoxic or hypoxic water (7.5% air saturation). Invasion, dissemination, and metastasis of DiI-tumor cells as well as tumor angiogenesis under normoxia or hypoxia were monitored daily in living zebrafish embryos.

Hypoxia Promotes Tumor Cell Metastasis. At day 3 after implantation, murine T241 tumor cells under hypoxia were significantly disseminated away from primary sites (Fig. 1 *D–F*), whereas virtually all tumor cells under normoxia remained at the primary sites (Fig. 1 *A–C*). In tumor-bearing fish embryos,

Author contributions: S.L.C.L., P.R., P.I., and Y.C. designed research; S.L.C.L. and P.R. performed research; S.L.C.L., L.D.J., D.Z., H.J., and G.H. contributed new reagents/analytic tools; S.L.C.L., P.R., and Y.C. analyzed data; and S.L.C.L., P.R., and Y.C. wrote the paper.

The authors declare no conflict of interest.

This article is a PNAS Direct Submission.

[1]S.L.C.L. and P.R. contributed equally to this work.

[2]To whom correspondence should be addressed. E-mail: yihai.cao@ki.se.

This article contains supporting information online at www.pnas.org/cgi/content/full/0909228106/DCSupplemental.

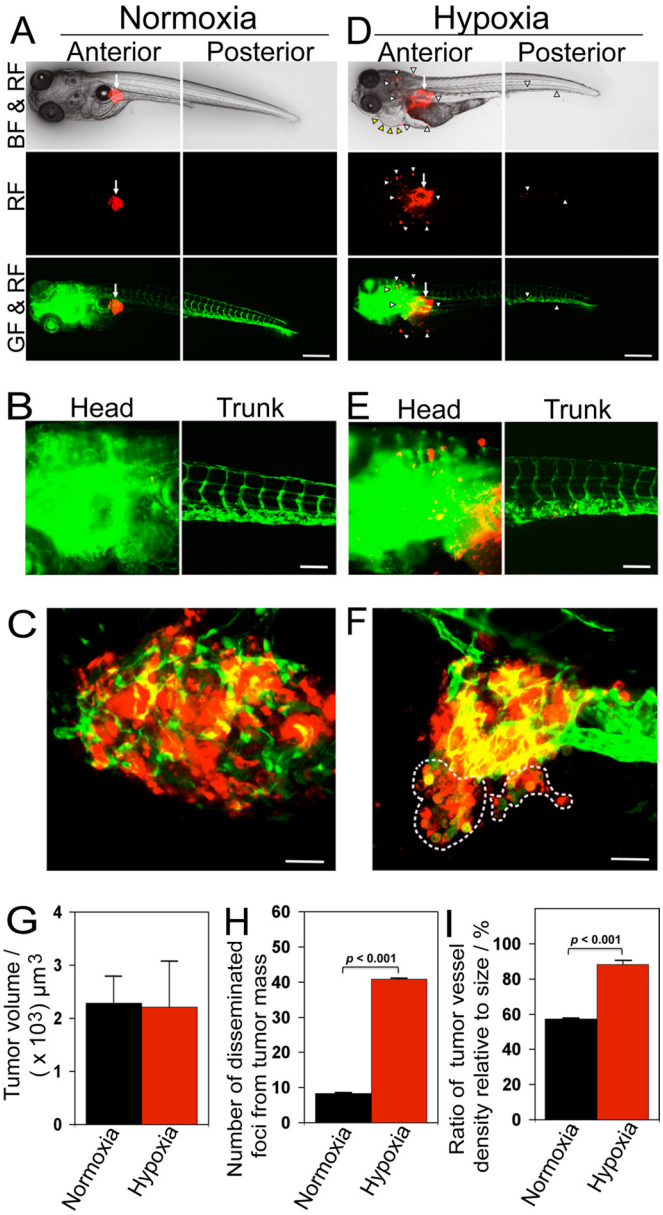

Fig. 1. Hypoxia promotes T241 tumor cell invasion, dissemination and metastasis. (*A* and *D*) DiI-labeled T241 tumor cells were injected into the perivitelline space of 48 h post-fertilization embryos and tumor cell invasion, dissemination and metastasis were detected under normoxia and hypoxia using fluorescent microscopy at day 3 post-injection. Arrows indicate primary tumors. Yellow arrowheads indicate pericardium edema. White arrowheads indicate disseminated tumor foci. (Scale bar, 500 μm.) (*B* and *E*) High-resolution micrographs of *A* and *D*, respectively. (Scale bar, 100 μm.) (*C* and *F*) Representative 3-D micrographs of confocal images of tumors (red) and tumoral as well as peritumoral vasculatures (green). Yellow signals show the intratumoral microvessels overlapping with tumor cells. Dashed lines encircle invasive fronts of T241 tumors under hypoxia. (Scale bar, 10 μm.) (*G*) Quantification of tumor volume (n = 13/group). (*H*) Quantification of numbers of disseminated tumor foci (n = 13/group). (*I*) Quantification of tumor vessel density relative to tumor sizes (n = 7/group). Data are represented as mean ± SEM.

the sizes of primary tumors in both groups remained similar (Fig. 1 *A–G*). The border of primary tumors under hypoxia was irregular and invasive fronts were often present (Fig. 1 *D–F*). In contrast, primary tumors under normoxia were restricted to the primary sites and lacked obvious signs of invasion (Fig. 1 *A* and *C*). In addition to local invasion, a substantial number of tumor cells under hypoxia were disseminated to distal parts of the fish body, including the head and tail regions (Fig. 1 *D* and *E*). High-resolution image analysis allowed us to detect single tumor cells in distal parts of the fish body (Fig. 1*E*). Under hypoxia, tumor-bearing zebrafish embryos suffered from tissue edema in the pericardium (Fig. 1*D*). Quantification analysis showed that significant high numbers of disseminated tumor foci were present in the hypoxic group relative to those in the control group (Fig. 1*H*).

Consistent with increase of tumor cell dissemination, hypoxia significantly stimulated neovascularization and tortuosity of the tumor vasculature (Fig. 1 *D–F* and *I*). In contrast, only a modest level of tumor neovascularization was detectable in fish embryos exposed to normoxia (Fig. 1 *A–C* and *I*). These findings demonstrate that hypoxia induces tumor angiogenesis, tumor cell dissemination, and metastasis in zebrafish.

In addition to T241 fibrosarcoma, we also studied hypoxia-induced tumor cell dissemination and metastasis in another murine tumor cell line, Lewis lung carcinoma (LLC). Similar to T241 fibrosarcoma, hypoxia substantially promoted tumor cell invasion, dissemination and metasatsis (Fig. S2). At day 3 post-implantation, considerable LLC tumor cells were disseminated to distal parts of the fish body and increase of tumor dissemination was well correlated with enhanced tumor neovascularization.

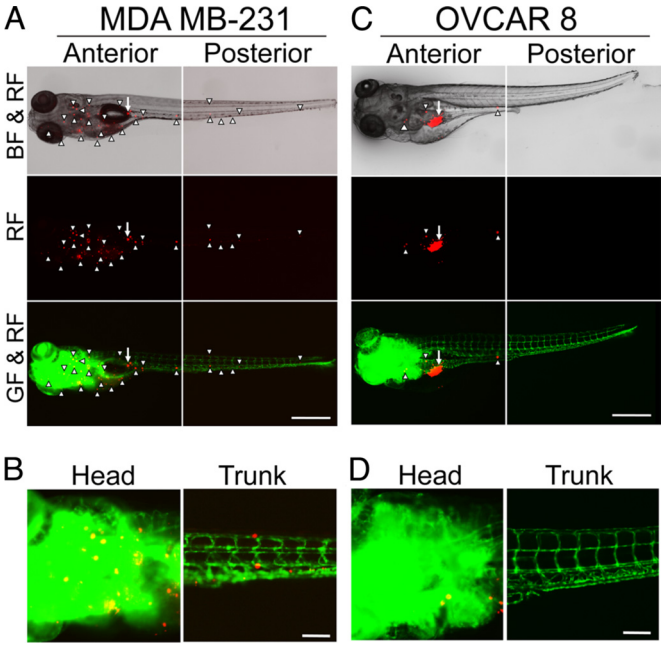

Fig. 2. Dissemination and metastasis of human tumor cells in zebrafish embryos. (*A* and *C*) Highly metastatic human MDA MB-231 breast and low metastatic human OVCAR 8 ovarian cancer cells were implanted into 48 h post-fertilization zebrafish embryos. Tumor cell dissemination and metastasis were detected at day 6 post-injection. Arrows indicate primary tumors and arrowheads indicate disseminated tumor foci. (Scale bar, 500 μm.) (*B* and *D*) High-resolution micrographs of *A* and *C*, respectively to visualize single metastatic tumor cells in the trunk regions. (Scale bar, 100 μm.)

Dissemination and Metastasis of Human Tumor Cells. To study the pathophysiological relevance of early events of the metastatic cascade in human tumors, we selected highly metastatic MDA MB-231 breast cancer and low metastatic OVCAR 8 ovarian cancer cell lines (23, 24). Interestingly, implantation of MDA MB-231 breast cancer cells in zebrafish embryos resulted in widespread tumor cell dissemination and metastasis at day 6 post-injection (Fig. 2 *A* and *B*). Markedly, virtually all MDA MB-231 tumor cells were

spread away from the primary site. In contrast, implantation of the low metastatic human OVCAR 8 ovarian cancer cells in zebrafish embryos did not result in significant dissemination and invasion (Fig. 2 *C* and *D*). Our results show that the difference of metastatic potentials between these two cell lines is due to their different capacities of dissemination, which is the earliest step of cancer metastasis. These findings demonstrate that our zebrafish metastasis model is highly relevant to recapitulation of clinical situation of metastasis. Thus, this zebrafish model might be used to discriminate high and low metastatic potentials of human cancers and to predict prognosis.

Tumor-Derived VEGF Facilitates Dissemination and Metastasis. Hypoxia is known to induce angiogenesis mainly via activation of the hypoxia inducible factor (HIF)-VEGF pathway. To study if VEGF could also promote tumor cell dissemination and metastasis, T241 tumor cells were stably transfected to express VEGF at a high level (25, 26). Similar to hypoxia, implantation of T241-VEGF tumor cells in developing zebrafish embryos led to extensive dissemination of tumor cells (Fig. 3 *D–F*). Local invasion and distal metastases were detectable in T241-VEGF tumor-bearing zebrafish embryos, but not in the control group (Fig. 3 *A–C*, *H*, and *I*). Quantification analysis showed while sizes of primary tumors were similar in both groups (Fig. 3*G*), total numbers of disseminated tumor cells and the maximal distance of metastasis in the T241-VEGF group were significantly greater than those in controls (Fig. 3 *H* and *I*). Similarly, microvessel density in T241-VEGF tumors was significantly higher relative to control tumors (Fig. 3*J*).

Time course analysis showed dissemination and invasion of T241-VEGF tumor cells occurred at a very early time point. At day 2 after implantation, a significant number of tumor cells invaded the neighboring tissues around primary tumors. At day 4, increasing numbers of invasive tumor cells were detected and were disseminated to distal parts of the fish body. Notably, tumor cell dissemination and metastasis were correlated with increased levels of tumor neovascularization. In contrast, T241-vector tumor-bearing zebrafish embryos lacked obvious tumor cell invasion, dissemination, and metastasis (Fig. S3).

To generalize these findings to other tumor types, murine LLC were also stably transfected with VEGF. Similar to T241 fibrosarcoma, implantation of LLC-VEGF tumors resulted in marked increase of tumor cell dissemination, invasion and distal metastasis compared with vector controls. LLC-VEGF but not LLC-vector tumor-bearing zebrafish embryos also exhibited tissue edema in the pericardium, indicating that the implanted tumor cells actively secreted functional VEGF molecules in the zebrafish body (Fig. S4). In positive correlation with tumor cell dissemination and metastasis, LLC-VEGF primary tumors were hypervascularized by high densities of disorganized and primitive vascular networks. In contrast, LLC-vector control primary tumors contained dispersed tumor blood vessels that were separated from each other (Fig. S4). These findings demonstrate that tumor cell-derived VEGF significantly contributes to the early dissemination of malignant cells, invasiveness and metastasis by promoting pathological angiogenesis.

VEGF Blockade Inhibits VEGF-Tumor Cell Invasion, Dissemination, and Metastasis. To further investigate the role of VEGF in mediating tumor cell invasion, dissemination, and metastasis, T241-VEGF tumor-bearing embryos were treated with sunitinib, a known VEGFR blockade (27, 28). Intriguingly, sunitinib effectively blocked tumor cell invasion, dissemination and metastasis (Fig. 4*A*). Consistent with the inhibition of tumor cell dissemination and metastasis, sunitinib also sufficiently blocked neovascularization in primary tumors (Fig. 4*B*). In fact, substantial tumor areas completely lacked detectable levels of microvessels in the sunitinib-treated zebrafish embryos (Fig. 4*B*). Quantification analysis showed that tumor cell dissemination, metastasis and vessel density in primary tumors were significantly inhibited by sunitinib in a dose-dependent manner (Fig. 4 *D–F*). Expectedly, the average size of primary tumors was also significantly reduced by sunitinib treatment. Similar to T241 fibrosarcoma, sunitinib effectively inhibited tumor cell dissemination and metastasis in LLC tumors (Fig. S5). These data demonstrate that anti-VEGF drugs such as sunitinib significantly inhibit tumor cell dissemination and metastasis.

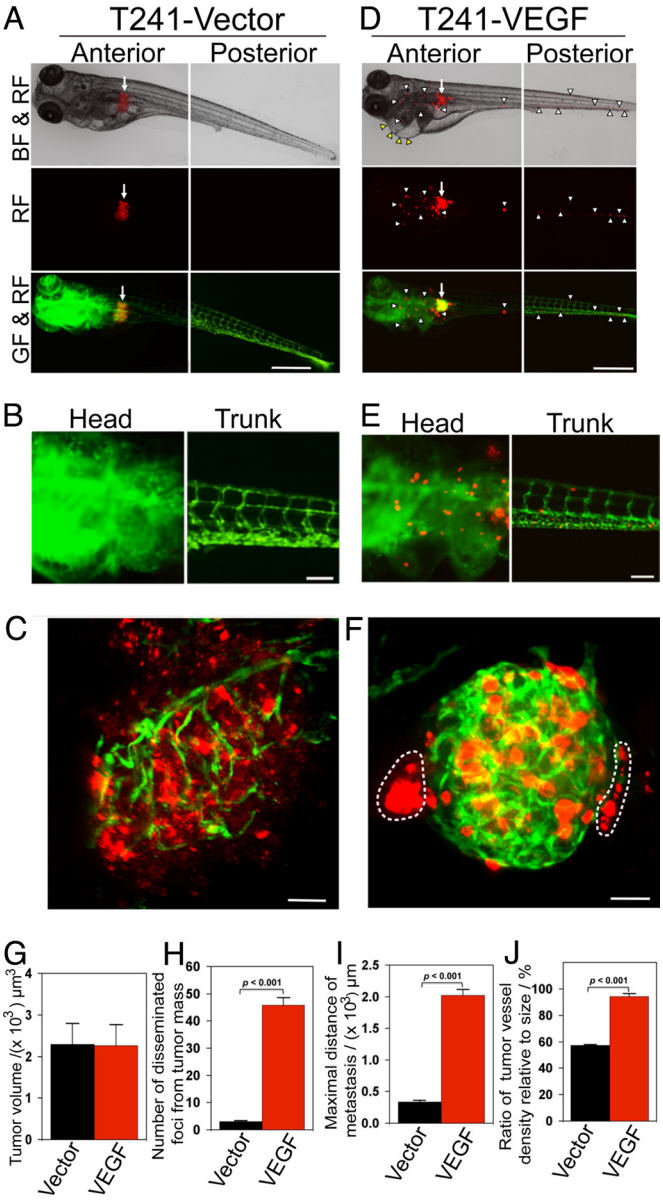

Fig. 3. Invasion, dissemination and metastasis of T241-VEGF tumors. (*A* and *D*) DiI-labeled T241-vector and T241-VEGF tumor cells were implanted in the perivitelline space and tumor cell invasion and dissemination were examined at day 6 post-injection. Arrows indicate primary tumors. Yellow arrowheads indicate pericardium edema. White arrowheads indicate disseminated tumor foci. (Scale bar, 500 μm.) (*B* and *E*) High-resolution micrographs of *A* and *D*, respectively to visualize single metastatic tumor cells. (Scale bar, 100 μm.) (*C* and *F*) Representative 3-D micrographs of confocal images of tumors (red) and tumor vasculatures (green). Dashed lines encircle invasive fronts of T241-VEGF tumors. (Scale bar, 10 μm.) (*G*) Quantification of tumor volume (n = 14/group). (*H*) Quantification of numbers of disseminated tumor foci (n = 14/group). (*I*) Averages of maximal distances of metastatic foci (n = 14/group). (*J*) Quantification of tumor vessel density relative to tumor sizes (n = 7/group). Data are represented as mean ± SEM.

MEDICAL SCIENCES

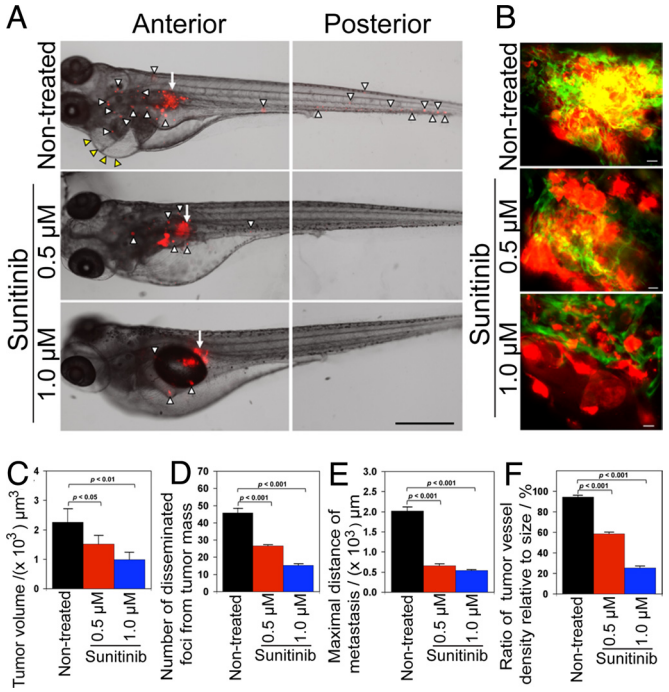

Fig. 4. Inhibition of tumor cell invasion, dissemination and metastasis by sunitinib. (*A*) Representative zebrafish embryos treated with or without 0.5 and 1.0 μM sunitinib. Arrows indicate primary tumors and arrowheads indicate disseminated and metastatic tumor cells in the distal parts of the fish body. (Scale bar, 500 μm.) (*B*) Representative 3-D micrographs of confocal images of tumors (red) and tumor vasculatures (green) in sunitinib-treated and non-treated groups. (Scale bar, 10 μm.) (*C*) Quantification of tumor volume (n = 10/group). (*D*) Quantification of disseminated tumor foci (n = 10/group). (*E*) Averages of maximal distances of metastatic foci (n = 10/group). (*F*) Quantification of tumor vessel density relative to tumor sizes (n = 7/group). Data are represented as mean ± SEM.

Inhibition of Tumor Cell Invasion, Dissemination, and Metastasis by VEGFR-2 Morpholinos. To further delineate the role of VEGF-induced signaling pathways in tumor angiogenesis, invasion, and metastasis, a specific morpholino against VEGFR-2, a functional receptor for VEGF-induced angiogenesis, was microinjected into developing zebrafish embryos (29, 30). Markedly, this specific morpholino virtually completely blocked VEGF-induced tumor cell dissemination, invasion, and metastasis (Fig. 5 *D–I*). In contrast, administration of an inert standard control morpholino (31) did not affect VEGF-induced tumor cell dissemination (Fig. 5 *A–C*). Consistent with suppression of tumor cell invasion and metastasis, the VEGFR-2 specific morpholino effectively blocked tumor angiogenesis (Fig. 5 *F* and *J*). It should be emphasized that administration of high dosages of VEGFR-2 morpholinos resulted in early death of zebrafish embryos owing to the essential role of VEGF in development of embryonic vasculatures as seen in mice (32, 33). At a relatively low concentration (0.1 mM), the VEGFR-2 morpholino selectively blocked tumor angiogenesis without significantly impairing development of physiological vascular networks, suggesting that the tumor vasculature was more susceptible to VEGF inhibition.

VEGFR Blockade Effectively Blocks Hypoxia-Induced Tumor Angiogenesis and Metastasis. Although hypoxia is known to increase tumor cell invasion and metastasis, the role of hypoxia-induced angiogenesis in mediation of tumor cell dissemination and metastasis remained elusive. Our hypoxic zebrafish tumor model offers an opportunity to study hypoxia-induced angiogenesis in promoting tumor cell dissemination and metastasis. Intriguingly, sunitinib

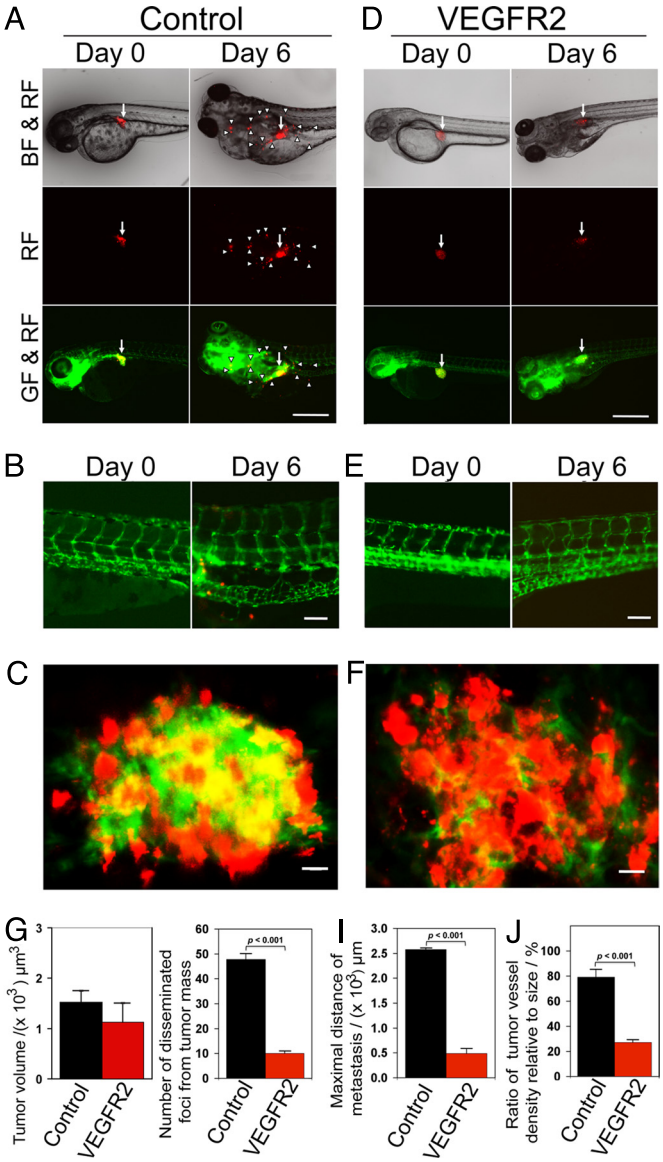

Fig. 5. Inhibition of tumor cell invasion, dissemination and metastasis by VEGFR2 morpholinos. (*A* and *D*) VEGFR2 specific morpholinos and control morpholinos were injected into the blastoma of 1 h post-fertilization at 1–4-cell stages. DiI-labeled T241-VEGF tumor cells were implanted in the perivitelline space of 48 h post-fertilization embryos and tumor cell invasion, dissemination and metastasis were detected at days 0 and 6 post-injection. White arrowheads indicate disseminated tumor foci. (Scale bar, 500 μm.) (*B* and *E*) High-resolution micrographs of *A* and *D*, respectively to visualize single metastatic tumor cells in the trunk regions. (Scale bar, 100 μm.) (*C* and *F*) Representative 3-D micrographs of confocal images of tumors (red) and tumor vasculatures (green). (Scale bar, 10 μm.) (*G*) Quantification of tumor volume (n = 12/group). (*H*) Quantification of numbers of disseminated tumor foci (n = 12/group). (*I*) Averages of maximal distances of metastatic foci (n = 12/group). (*J*) Quantification of tumor vessel density relative to tumor size (n = 7/group). Data are represented as mean ± SEM.

virtually completely blocked the hypoxia-induced T241 tumor cell invasion, dissemination and metastasis (Fig. 6 *A–H*). Consistent with inhibition of tumor cell invasion and metastasis, sunitinib significantly inhibited tumor neovascularization (Fig. 6 *C*, *F*, and *H*). These results provide compelling evidence that hypoxia-induced malignant cell invasion, dissemination, and metastasis are mediated by VEGF-induced pathological blood vessels.

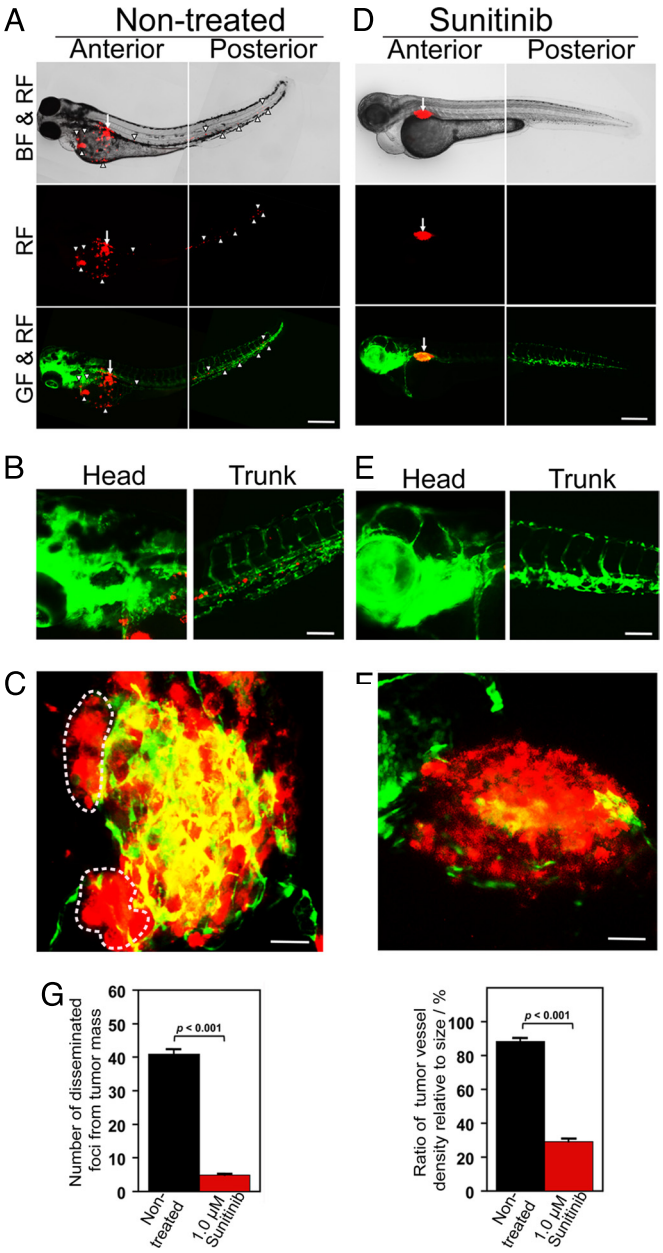

Fig. 6. Sunitinib inhibits hypoxia-induced invasion, dissemination and metastasis of T241 tumors. (*A* and *D*) DiI-labeled T241 tumor cells were implanted in the perivitelline space of 48 h post-fertilization embryos and shortly after injection zebrafish embryos were placed into a hypoxic chamber containing 7.5% air saturation, immediately followed by treatment with 1.0 μM sunitinib. Tumor cell invasion, dissemination and metastasis were detected at day 3 post-injection. Arrows indicate primary tumors and arrowheads indicate disseminated tumor foci. (Scale bar, 500 μm.) (*B* and *E*) High-resolution micrographs of *A* and *D*, respectively to visualize single metastatic tumor cells in the trunk regions. (Scale bar, 100 μm.) (*C* and *F*) Representative 3-D micrographs of confocal images of tumors (red) and tumor vasculatures (green). Dashed lines encircle invasive fronts of T241 tumors. (Scale bar, 10 μm.) (*G*) Quantification of numbers of disseminated tumor foci (n = 11/group). (*H*) Quantification of tumor vessel density relative to tumor sizes (n = 7/group). Data are represented as mean ± SEM.

Discussion

Metastasis is one of the hallmarks of malignant diseases and causes the death of majority of cancer patients (34). Once a solid tumor spreads to other tissues and organs, curative intervention with currently available cancer drugs, surgical operation, and radiotherapy are ineffective. Thus, early detection of malignant tumors is essential for curative therapy. However, cancer metastasis can occur at the very early stage of malignant diseases and in a substantial number of cases metastatic disease is the first sign of cancer whereas primary tumors remain undetectable (35, 36). Molecular mechanisms underlying the early onset of cancer metastasis are complex, which involve in both genetic and epigenetic alterations in malignant cells and the tumor environment. Sequential genetic events in malignant cells might lead to invasion and metastasis. For example, mutations of p53 lead to inactivation of p63 and trigger a TGF-β-dependent invasive and metastatic phenotype (37). To the best of our knowledge, the role of angiogenesis in tumor cell dissemination has not been well-described in mammalian tumor models.

A clinically detectable metastasis represents the end point of the metastatic cascade that consists of distinct steps, including tumor cell dissemination from the primary site, transport of malignant cells via blood or lymphatic systems, formation of new tumor niches in remote tissues and organs, and re-growth of metastatic niches into a clinically detectable mass. Current preclinical animal models and clinical detection techniques do not allow studying the early events of the metastatic cascade. To recapitulate early steps of clinical metastasis, we develop a zebrafish metastatic model that allows us to monitor dissemination of single tumor cells from primary sites in the living body. This metastasis model has several features and advantages over other existing models in mice. These include: 1) The transparent nature of zebrafish embryos allows us to monitor tumor development and dissemination in vivo without any invasive operation; 2) EGFP positive vasculature in *fli1:EGFP* zebrafish embryos further permit us to study tumor cell dissemination in relation to development of angiogenic vessels; 3) Zebrafish could easily be placed in hypoxic water to study the role of tissue hypoxia in facilitating tumor cell dissemination and metastasis (38); 4) Assessment of anti-metastatic effects of orally active drugs; and 5) Morpholino for reverse genetics by silencing host gene functions involving angiogenesis and metastasis (39). These advantages offer an opportunity to study molecular mechanisms of tumor cell invasion, dissemination, and metastasis in association to angiogenesis and hypoxia in vivo.

Tissue hypoxia significantly contributes to tumor invasion and metastasis by mechanisms of altering malignant cell motility, migration, invasiveness, and angiogenesis (40). Recently, it has been shown that anti-VEGF drugs can also induce tumor cell invasion and metastasis in association with antiangiogenesis-induced tissue hypoxia. It is generally believed that antiangiogenic drug-induced hypoxia in the tumor environment persuade malignant cells to invade neighboring healthy vasculatures for survival and spread. However, significant improvement of patient survivals by antiangiogenic drugs argues against dreadful effects of these drugs for treatments of various cancers (41–43). In the present study, we demonstrate that hypoxia significantly increases tumor cell dissemination by activation of VEGF and its receptor-mediated signaling pathway. Similar to hypoxia, stable expression of VEGF in tumor cells substantially facilitates tumor cell invasion, dissemination and metastasis. Because tumor cells lack VEGF receptor expression and responses, these findings show that tumor angiogenesis plays an essential role in arbitrating tumor cell invasion and dissemination. How does VEGF-induced angiogenesis facilitate tumor cell invasion and metastasis? One possibility is that VEGF induces disorganized, leaky and tortuous vasculatures, which are susceptible for malignant cell invasion. In support of this hypothesis, increases of vascular density and tortuosity have been observed in our zebrafish model. The other possible mechanism is that outgrowth of blood vessels in tumors promotes intimate interactions between malignant and endothelial cells and the latter provides niches for tumor cell invasion and metastasis. Additionally, perfusion of VEGF-induced vessels could act as a chemoattractant for tumor

cell migration and eventually lead to tumor cell invasion along the vascular system.

Dissemination of tumor cells from the primary site is the initial step of the metastatic cascade and inhibition of this process is probably the most effective approach for cancer therapy. The prerequisite role of tumor angiogenesis in disseminating malignant cells shown in the present study suggests that inhibition of tumor angiogenesis might prevent metastasis. Inversely, recent reports show that antiangiogenic drugs for treatment of established animal tumors lead to invasion and metastasis. The difference between these findings and our data could be due to the sizes of primary tumors. In an established tumor, anti-VEGF drugs could generate tissue hypoxia, leading to an invasive and metastatic phenotype. In our zebrafish tumor model, primary tumors remain in situ as tiny nodules and antiangiogenic drugs would not result in significant hypoxia as in a well-established tumor. Thus, tumor sizes might be a key determinant for antiangiogenic drug-produced therapeutic benefits or tumor cell invasion and metastasis.

Our findings show that dissemination of tumor cells occurs while primary tumors are relatively small is highly relevant to clinical situations. A substantial number of patients are diagnosed for malignant diseases owing to metastasis as the first sign of cancer. In these cases, primary tumors remain undetectable using conventional techniques, suggesting that dissemination of tumor cells occurs at the very early stage. Thus, our results shed light on early metastatic processes by visualizing single cell invasion and metastasis in the living body without invasive procedures. Understanding molecular mechanisms of angiogenesis- and tissue hypoxia-induced tumor cell invasion and metastasis has conceptual implications for treatments of metastatic disease.

Materials and Methods

Zebrafish Tumor Model. All experimental procedures of zebrafish research were approved by the Northern Stockholm Experimental Animal Ethical Committee. Detailed methods of microinjection are described in *SI Materials and Methods*.

Cell Culture. Cells were kept and grown in DMEM supplemented with 10% FBS (FBS). See *SI Materials and Methods* for details.

Anti-VEGF Treatment. Orally active VEGFR tyrosine kinase inhibitor, sunitinib (LC Laboratories) was dissolved in dimethyl sulfoxide (DMSO) to make a stock solution of 10 mM. See *SI Materials and Methods* for details.

Morpholino Treatment. Morpholino oligonucleotides (MOs) were obtained from Gene Tools. See *SI Materials and Methods* for details.

Zebrafish Hypoxia Experiment. The zebrafish hypoxia system was established according to our previously published procedure (38). See *SI Materials and Methods* for details.

Statistical Analysis. Statistical analysis was performed using the Student's *t*-test by a Microsoft Excel program. Data were presented as means of determinants (± SEM) and P values <0.05 were considered as statistically significant.

ACKNOWLEDGMENTS. This work was supported by the laboratory of Y.C. through research grants from the Swedish Research Council, the Swedish Heart and Lung Foundation, the Swedish Cancer Foundation, the Karolinska Institute Foundation, the Torsten and Ragnar Söderberg's Foundation, and European Union Integrated Projects of Angiotargeting Contract 504743 (to Y.C.) and VascuPlug Contract STRP 013811 (to Y.C.). We thank the Biomedical Research Council of the Agency for Science, Technology and Research (A*STAR), Singapore for awarding S.L.C.L. the PhD scholarship. Y.C. is a Chang Jiang Scholar at the Shandong University, China.

1. Folkman J (1971) Tumor angiogenesis: Therapeutic implications. *N Engl J Med* 285:1182–1186.
2. Weidner N, Semple JP, Welch WR, Folkman J (1991) Tumor angiogenesis and metastasis–correlation in invasive breast carcinoma. *N Engl J Med* 324:1–8.
3. Cao Y (2009) Tumor angiogenesis and molecular targets for therapy. *Front Biosci* 14:3962–3973.
4. Carmeliet P, Jain RK (2000) Angiogenesis in cancer and other diseases. *Nature* 407:249–257.
5. Jain RK (2005) Normalization of tumor vasculature: An emerging concept in antiangiogenic therapy. *Science* 307:58–62.
6. Kerbel RS (2008) Tumor angiogenesis. *N Engl J Med* 358:2039–2049.
7. Heldin CH, Rubin K, Pietras K, Ostman A (2004) High interstitial fluid pressure-an obstacle in cancer therapy. *Nat Rev Cancer* 4:806–813.
8. Bhandarkar SS, et al. (2009) Fulvene-5 potently inhibits NADPH oxidase 4 and blocks the growth of endothelial tumors in mice. *J Clin Invest* 119:2359–2365.
9. Blagosklonny MV (2004) Antiangiogenic therapy and tumor progression. *Cancer Cell* 5:13–17.
10. Du R, et al. (2008) HIF1alpha induces the recruitment of bone marrow-derived vascular modulatory cells to regulate tumor angiogenesis and invasion. *Cancer Cell* 13:206–220.
11. Erler JT, et al. (2009) Hypoxia-induced lysyl oxidase is a critical mediator of bone marrow cell recruitment to form the premetastatic niche. *Cancer Cell* 15:35–44.
12. Nikolopoulos SN, Blaikie P, Yoshioka T, Guo W, Giancotti FG (2004) Integrin beta4 signaling promotes tumor angiogenesis. *Cancer Cell* 6:471–483.
13. Wei J, et al. (2004) Embryonic endothelial progenitor cells armed with a suicide gene target hypoxic lung metastases after intravenous delivery. *Cancer Cell* 5:477–488.
14. Kerbel RS (2006) Antiangiogenic therapy: A universal chemosensitization strategy for cancer? *Science* 312:1171–1175.
15. Paez-Ribes M, et al. (2009) Antiangiogenic therapy elicits malignant progression of tumors to increased local invasion and distant metastasis. *Cancer Cell* 15:220–231.
16. Ebos JM, et al. (2009) Accelerated metastasis after short-term treatment with a potent inhibitor of tumor angiogenesis. *Cancer Cell* 15:232–239.
17. Pantel K, Brakenhoff RH (2004) Dissecting the metastatic cascade. *Nat Rev Cancer* 4:448–456.
18. Boutin AT, et al. (2008) Epidermal sensing of oxygen is essential for systemic hypoxic response. *Cell* 133:223–234.
19. Mandriota SJ, et al. (2002) HIF activation identifies early lesions in VHL kidneys: Evidence for site-specific tumor suppressor function in the nephron. *Cancer Cell* 1:459–468.
20. Bruick RK, McKnight SL (2001) A conserved family of prolyl-4-hydroxylases that modify HIF. *Science* 294:1337–1340.
21. Semenza GL (2001) HIF-1, O(2), and the 3 PHDs: How animal cells signal hypoxia to the nucleus. *Cell* 107:1–3.
22. Lawson ND, Weinstein BM (2002) In vivo imaging of embryonic vascular development using transgenic zebrafish. *Dev Biol* 248:307–318.
23. Miao J, et al. (2007) HOXB13 promotes ovarian cancer progression. *Proc Natl Acad Sci USA* 104:17093–17098.
24. Yin JJ, et al. (1999) TGF-beta signaling blockade inhibits PTHrP secretion by breast cancer cells and bone metastases development. *J Clin Invest* 103:197–206.
25. Eriksson A, et al. (2002) Placenta growth factor-1 antagonizes VEGF-induced angiogenesis and tumor growth by the formation of functionally inactive PlGF-1/VEGF heterodimers. *Cancer Cell* 1:99–108.
26. Xue Y, et al. (2008) Anti-VEGF agents confer survival advantages to tumor-bearing mice by improving cancer-associated systemic syndrome. *Proc Natl Acad Sci USA* 105:18513–18518.
27. Billemont B, Barete S, Rixe O (2008) Scrotal cutaneous side effects of sunitinib. *N Engl J Med* 359:975–976.
28. Motzer RJ, et al. (2007) Sunitinib versus interferon alfa in metastatic renal-cell carcinoma. *N Engl J Med* 356:115–124.
29. Rottbauer W, et al. (2005) VEGF-PLCgamma1 pathway controls cardiac contractility in the embryonic heart. *Genes Dev* 19:1624–1634.
30. Nicoli S, Presta M (2007) The zebrafish/tumor xenograft angiogenesis assay. *Nat Protoc* 2:2918–2923.
31. Lee P, et al. (2002) Neuropilin-1 is required for vascular development and is a mediator of VEGF-dependent angiogenesis in zebrafish. *Proc Natl Acad Sci USA* 99:10470–10475.
32. Carmeliet P, et al. (1996) Abnormal blood vessel development and lethality in embryos lacking a single VEGF allele. *Nature* 380:435–439.
33. Ferrara N, et al. (1996) Heterozygous embryonic lethality induced by targeted inactivation of the VEGF gene. *Nature* 380:439–442.
34. Hanahan D, Weinberg RA (2000) The hallmarks of cancer. *Cell* 100:57–70.
35. Husemann Y, et al. (2008) Systemic spread is an early step in breast cancer. *Cancer Cell* 13:58–68.
36. Aguirre-Ghiso JA (2007) Models, mechanisms and clinical evidence for cancer dormancy. *Nat Rev Cancer* 7:834–846.
37. Adorno M, et al. (2009) A Mutant-p53/Smad complex opposes p63 to empower TGFbeta-induced metastasis. *Cell* 137:87–98.
38. Cao R, Jensen LD, Soll I, Hauptmann G, Cao Y (2008) Hypoxia-induced retinal angiogenesis in zebrafish as a model to study retinopathy. *PLoS ONE* 3:e2748.
39. Nasevicius A, Ekker SC (2000) Effective targeted gene 'knockdown' in zebrafish. *Nat Genet* 26:216–220.
40. Holmquist-Mengelbier L, et al. (2006) Recruitment of HIF-1alpha and HIF-2alpha to common target genes is differentially regulated in neuroblastoma: HIF-2alpha promotes an aggressive phenotype. *Cancer Cell* 10:413–423.
41. Bose P, Holter JL, Selby GB (2009) Bevacizumab in hereditary hemorrhagic telangiectasia. *N Engl J Med* 360:2143–2144.
42. Haines IE, Miklos GL (2008) Paclitaxel plus bevacizumab for metastatic breast cancer. *N Engl J Med* 358:1637–1638.
43. Sculier JP, Meert AP, Paesmans M (2007) Bevacizumab for non-small-cell lung cancer. *N Engl J Med* 356:1373–1374.